



## UvA-DARE (Digital Academic Repository)

### Selective Carbanion-Pyridine Coordination of a Reactive P,N Ligand to Rh-I

Devillard, M.; Ehlers, A.; Siegler, M.A.; van der Vlugt, J.I.

**DOI**

[10.1002/chem.201805504](https://doi.org/10.1002/chem.201805504)

**Publication date**

2019

**Document Version**

Final published version

**Published in**

Chemistry-A European Journal

**License**

CC BY-NC-ND

[Link to publication](#)

**Citation for published version (APA):**

Devillard, M., Ehlers, A., Siegler, M. A., & van der Vlugt, J. I. (2019). Selective Carbanion-Pyridine Coordination of a Reactive P,N Ligand to Rh<sup>I</sup>. *Chemistry-A European Journal*, 25(15), 3875-3883. <https://doi.org/10.1002/chem.201805504>

**General rights**

It is not permitted to download or to forward/distribute the text or part of it without the consent of the author(s) and/or copyright holder(s), other than for strictly personal, individual use, unless the work is under an open content license (like Creative Commons).

**Disclaimer/Complaints regulations**

If you believe that digital publication of certain material infringes any of your rights or (privacy) interests, please let the Library know, stating your reasons. In case of a legitimate complaint, the Library will make the material inaccessible and/or remove it from the website. Please Ask the Library: <https://uba.uva.nl/en/contact>, or a letter to: Library of the University of Amsterdam, Secretariat, Singel 425, 1012 WP Amsterdam, The Netherlands. You will be contacted as soon as possible.

## Coordination Modes | Hot Paper |

Selective Carbanion–Pyridine Coordination of a Reactive P,N Ligand to Rh<sup>I</sup>Marc Devillard,<sup>[a]</sup> Andreas Ehlers,<sup>[a, b]</sup> Maxime A. Siegler,<sup>[c]</sup> and Jarl Ivar van der Vlugt\*<sup>[a]</sup>

**Abstract:** Ligands with reactive carbon sites in the periphery of a metal center have emerged as a powerful approach for metal–ligand bond activation. These reactive carbon sites are commonly generated by deprotonation strategies. Carbon–silicon bond cleavage is a potential alternative to access such constructs. Herein, the monodesilylation of bisilyl-substituted P,N scaffold **PN<sup>Si2</sup>** in the coordination sphere of [Rh<sup>I</sup>(Cl)(CO)(**PN<sup>Si2</sup>**)] (**1**) with sodium azide is disclosed. This affords a unique dinucleating anionic  $\kappa^2$ -C,N- $\kappa^1$ -P ligand with

a carbanionic methine carbon atom directly bound to rhodium as part of a four-membered Rh–N–C–C rhodacycle. This dimer undergoes *meta*-pyridine C–H activation facilitated by weak bases, which leads to a desymmetrization of the system and provides a  $\sigma,\pi$ -bridging 3-pyridyl fragment bound to Rh<sup>I</sup>. The facile Si–C cleavage strategy may pave the way to studying the reactivity and functionalization of a variety of  $\kappa^2$ -C,N-coordinated pyridine scaffolds for selective transformations.

## Introduction

Reactive ligands that are amenable to chemical changes in their backbone have recently attracted much attention in cooperative metal–ligand bifunctional substrate activation, particularly with late transition metals.<sup>[1]</sup> Lutidine-based platforms with a hybrid P,N donor set, either as tridentate<sup>[2–4]</sup> or bidentate ligand,<sup>[5]</sup> are often encountered in this context. Deprotonation of the acidic methylene linker between the pyridine and the flanking P donor atom with strong non-nucleophilic bases typically generates an exocyclic C=C bond with a neutral methine group and an anionic nitrogen donor through formal dearomatization of the N-heterocycle.<sup>[6]</sup> To date, with transition metals,<sup>[7]</sup> this typically gives rise to the ubiquitous amido(methine)phosphane P,N binding, wherein the methine carbon atom has no direct bonding interaction with the metal center (Figure 1). We surmised that C,N ligation could provide a

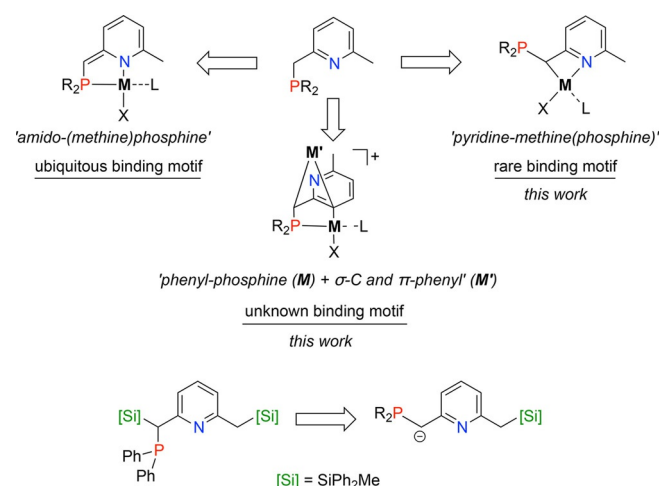


**Figure 1.** Top: Common reactivity of 2-lutidine-derived P,N ligands on dearomatization versus rare C,N binding motif and unprecedented dinucleating phenylphosphane +  $\eta^3$ -benzyl coordination. Bottom: envisioned selective monodesilylation strategy of a **PN<sup>Si2</sup>** ligand to generate a carbanionic methine.

highly attractive alternative scenario to further expand the chemistry of reactive ligands. Such coordination might change the energetics of substrate bond-activation pathways, depending on the M–C bond strength, and potentially offer new modes and pathways for reactivity. Starting with the ligand 2-(di-*tert*-butylphosphanyl)methyl-6-methylpyridine, selective C,N versus P,N binding, the former generating a strained four-membered metallacycle, was recently serendipitously observed for the first time for Group 13 complexes,<sup>[8]</sup> but no report on C,N binding to transition metals for such phosphino-pyridine ligands exists to date, as phosphane coordination to form a five-membered ring is typically preferred. Structurally related 2-aminopyridines are known to relatively easily afford  $\eta^2$ -N,N

[a] Dr. M. Devillard, Dr. A. Ehlers, Dr. Ir. J. I. van der Vlugt  
van 't Hoff Institute for Molecular Sciences, University of Amsterdam  
Science Park 904, 1098 XH Amsterdam (The Netherlands)  
E-mail: j.i.vandervlugt@uva.nl

[b] Dr. A. Ehlers  
Department of Chemistry, University of Johannesburg  
P.O. Box 254, Auckland Park, Johannesburg (South Africa)

[c] Dr. M. A. Siegler  
Department of Chemistry, Johns Hopkins University  
3400 N Charles Street, Baltimore, MD 21218 (USA)

Supporting information and the ORCID identification number(s) for the author(s) of this article can be found under:  
<https://doi.org/10.1002/chem.201805504>.

© 2019 The Authors. Published by Wiley-VCH Verlag GmbH & Co. KGaA. This is an open access article under the terms of Creative Commons Attribution NonCommercial-NoDerivs License, which permits use and distribution in any medium, provided the original work is properly cited, the use is non-commercial and no modifications or adaptations are made.

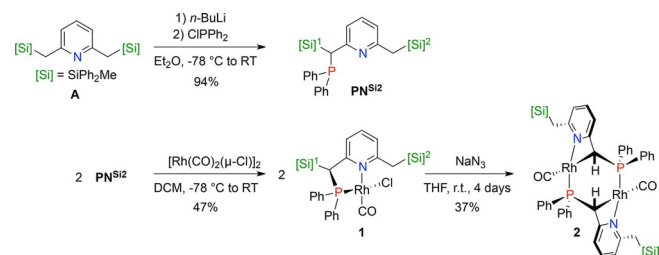
binding on deprotonation (resulting in an amidopyridinate donor),<sup>[9]</sup> but the related  $\eta^2$ -C,N binding motif is very rare for 2-methine pyridines and elusive for low-valent metal centers.<sup>[10]</sup> Stimulated by the development of related metal-bound monoanionic, neutral, or dianionic carbon-ligand fragments for bond-activation strategies<sup>[11]</sup> and our recent reports that Rh–C<sub>aryl</sub> bonds may be employed for bifunctional substrate activation,<sup>[12]</sup> we explored strategies to generate such transition metal–pyridine–carbanion structures.

To address this challenge, we envisioned that regioselective desilylation of a suitable functionalized *P,N* scaffold bearing diphenylmethylsilyl groups might offer an entry into this chemistry. This would result in the formation of a carbanionic methine linker without affecting the aromatization of the pyridine ring. Although carbon–silicon bond breaking has been reported for the construction of cyclometalated ligand frameworks and for organic synthesis,<sup>[13]</sup> site-selective C–Si bond cleavage in a disilylated platform has not been utilized for the generation of reactive ligand scaffolds to the best of our knowledge. We herein show that this selective side-arm desilylation concept provides access to the first example of selective carbanion-C over phosphorus-P binding to rhodium to produce a unique dinuclear rhodium complex stabilized by a dearomatized, anionic, and dinucleating NCP scaffold. This has provided the first example of a four-membered low-valent Rh<sup>I</sup>-N-C-C metallacycle as well as the first example of a transition metal center bound simultaneously to the methine carbon and the pyridine nitrogen atoms in these reactive *P,N*-type lutidine-based platforms.

## Results and Discussion

Bis-silyl-decorated *P,N* ligand **PN**<sup>Si2</sup> was synthesized straightforwardly by monodeprotonation of 2,6-bis[(diphenylmethylsilyl)methyl]pyridine (**A**)<sup>[14]</sup> with one equivalent of *n*BuLi, followed by addition of chlorodiphenylphosphane (Scheme 1). Desymmetrization of the bis(silyl)lutidine unit is reflected in the <sup>29</sup>Si NMR spectrum, which shows a doublet at  $\delta[\text{Si}]^1 = -8.2$  with an Si–P coupling constant <sup>2</sup>*J*<sub>SiP</sub> of 18.5 Hz and a singlet at slightly lower field [ $\delta[\text{Si}]^2 = -7.8$  (s)].

Coordination of **PN**<sup>Si2</sup> to 0.5 molar equivalents of  $[\{\text{Rh}(\text{CO})_2(\mu\text{-Cl})\}_2]$  resulted in yellow crystals in good yield after workup (Scheme 1). Multinuclear NMR and IR spectroscopic data (<sup>31</sup>P:  $\delta = 67.6$  ppm, <sup>1</sup>*J*<sub>RhP</sub> = 167.6 Hz; IR:  $\nu_{\text{CO}} = 1987$  cm<sup>-1</sup>) as



**Scheme 1.** Synthesis of mononuclear Rh<sup>I</sup> complex **1** and subsequent azide-induced selective desilylation to provide Rh<sup>I</sup> dimer **2** featuring two four-membered Rh–N–C–C metallacycles.

well as HRMS (FD;  $m/z = 849.12866$  [ $M$ ]<sup>+</sup>) support the formation of the anticipated mononuclear Rh<sup>I</sup> complex  $[\text{RhCl}(\text{CO})(\kappa^2\text{-P,N-PN}^{\text{Si2}})]$  (**1**) with *trans* disposition of Cl and P. The molecular structure as determined by XRD (Figure 2) shows significant

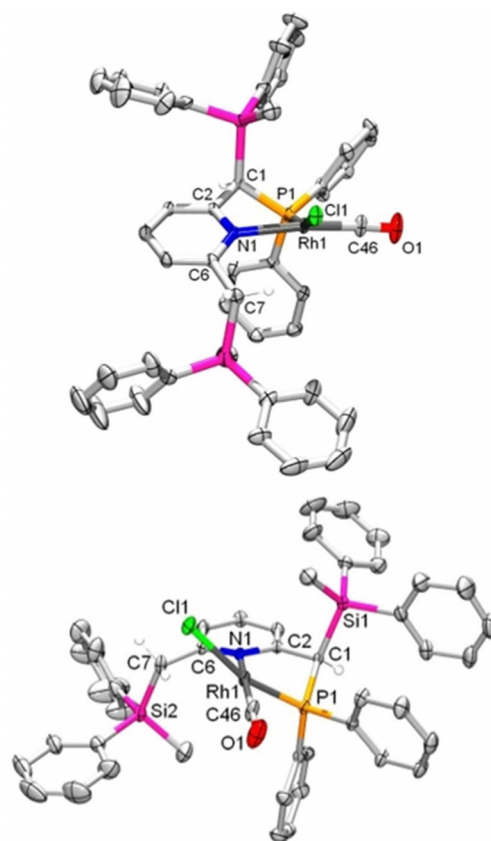


**Figure 2.** Displacement ellipsoid plots (50% probability) of **1** (top: side view; bottom: front view) at 150 K. Hydrogen atoms, apart from those on C1 and C7, are omitted for clarity. Selected bond lengths [Å] and angles [°]: Rh1–C46 1.804(3); C46–O1 1.147(3); Rh1–Cl1 2.4144(6); Rh1–N1 2.168(17); Rh1–P1 2.1943(6); P1–C1 1.847(2); C1–C2 1.510(3); C1–Si1 1.926(2); C7–Si2 1.895(3); C46–Rh1–N1 169.48(10); Cl1–Rh1–P1 163.71(2); N1–Rh1–C46 169.48(10); Rh1–P1–C1 98.75(7); P1–C1–Si1 119.46(11); P1–C1–C2 104.62(14); Cl1–Rh1–N1–C6 –47.1(2); C46–Rh1–P1–Cl1 –110.8(1); P1–Rh1–N1–Cl1 –164.09(3); N1–Rh1–P1–Cl1 76.3(1).

out-of-plane displacement of the chlorido ligand, with a P1–Rh1–Cl1 angle of 163.71(2)° and a C46–Rh1–P1–Cl1 torsion angle of –110.8(1)°. The <sup>1</sup>H NMR spectral data and DFT calculations<sup>[15]</sup> suggest the presence of an H-bonding interaction between the chlorido ligand and one of the methylene CH<sub>2</sub> hydrogen atoms of the nonsubstituted CH<sub>2</sub>Si(Ph<sub>2</sub>)(Me) arm in solution, resulting in a AB system with a large  $\Delta\nu_{\text{AB}}$  value of 697.5 Hz ( $\delta_{\text{A}} = 2.97$ ;  $\delta_{\text{B}} = 5.30$ ). In situ abstraction of the Cl ligand with AgSbF<sub>6</sub> resulted in a narrower AB system ( $\Delta\nu_{\text{AB}} = 126.0$  Hz,  $\delta_{\text{A}} = 2.76$ ;  $\delta_{\text{B}} = 3.18$ ).<sup>[16]</sup> This is likely related to the intrinsic acidity of lutidine C(sp<sup>3</sup>)H protons, which is further enhanced by the ability of silicon to undergo hyperconjugation to stabilize  $\alpha$ -carbanions.

To assess the possibility of inducing carbanion formation from complex **1**, its reactivity toward external silylium-abstraction agents was probed. Using fluoride sources such as tetra-

butylammonium fluoride or tetrabutylammonium difluorotriphenylsilicate led to instantaneous reactions (even at  $-78^{\circ}\text{C}$ ), but complicated reaction mixtures were obtained according to in situ  $^{31}\text{P}$  NMR spectroscopy. Switching to an excess of sodium azide as a less-reactive silicon-group acceptor led to quantitative conversion, judged by  $^{31}\text{P}$  NMR spectroscopy, and a change of color from yellow to dark brown. After workup, compound **2** was isolated as yellow needles in 37% yield. Its IR spectrum showed no evidence of an Rh–azido fragment but did contain a low-energy-shifted  $\nu_{\text{CO}}$  band at  $1947\text{ cm}^{-1}$  ( $\Delta\bar{\nu} = -40\text{ cm}^{-1}$  relative to **1**), suggesting a CO ligand *trans* to a strongly donating ligand. The  $^{31}\text{P}$  NMR spectrum contained only a single signal at  $\delta = 45.7$ , interpreted as a second-order AA'BB' spin system. Carbon–silicon bond cleavage, that is, removal of silyl group  $[\text{Si}]^{\beta}$  to phosphorus, was confirmed by  $^{29}\text{Si}$  and  $^1\text{H}$  NMR spectroscopy. Unfortunately, low resolution of the  $^{13}\text{C}$  NMR spectrum precluded definitive identification of the carbon center previously linked to silicon. However, the broadened  $^1\text{H}$  NMR signal at  $\delta = 2.33$ , attributed to the methine CHP hydrogen atom, is found far outside the olefinic region, which disagrees with the enamine form of the N heterocycle that would be generated on dearomatization of the pyridine ring.

Single crystals suitable for X-ray structure determination were obtained by layering a THF solution of **2** with pentane at RT (Figure 3). The resulting molecular structure indicates formation of a dinuclear complex, formulated as  $[\{\text{Rh}^{\text{I}}(\text{CO})(\kappa^2\text{-N,C};\kappa^1\text{-P-}\mu\text{-PN}^{\text{Si}})\}_2]$ . The methine carbon atom is directly linked to the adjacent rhodium center (Rh1–C1 2.137(6) Å) in favor of the phosphane P donor, and thus the formation of a strained four-membered ring fused with an aromatic N heterocycle is enforced<sup>[17]</sup> and a distorted square-planar geometry around Rh results [C1–Rh1–N1 65.7(2) $^{\circ}$ ,  $\Sigma\text{Rh}_{\text{angles}} = 360^{\circ}$ ]. The carbon–carbon distances in the heterocycle support aromatic nature of

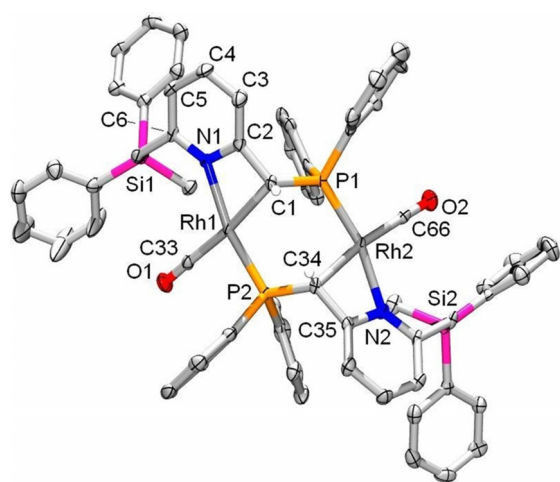
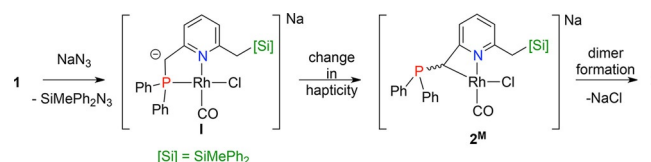


**Figure 3.** Displacement ellipsoid plots (50% probability) of **2** at 150 K. Hydrogen atoms, apart from those on C1 and C7, and THF lattice-solvent molecules are omitted for clarity. Selected bond lengths [Å] and angles [ $^{\circ}$ ]: Rh1–C33 1.840(6); C33–O1 1.157(7); Rh1–N1 2.096(4); Rh2–P1 2.230(1); Rh1–C1 2.137(6); P1–C1 1.805(6); C1–C2 1.492(5); C2–N1 1.360(6); C2–C3 1.377(7); C3–C4 1.390(5); C4–C5 1.391(8); C5–C6 1.387(7); C33–Rh1–P2 90.1(2); C33–Rh1–N1 105.9(2); P1–C1–Rh1 110.0(3); P2–Rh1–C1 98.3(1); C1–Rh1–N1 65.7(2); Rh1–C1–C2 90.4(3); C1–C2–N2 107.2(4); C2–N1–Rh1 96.0(3).

the pyridine ring. Combined with the only marginally shorter C1–C2 bond length relative to complex **1** ( $\Delta d = 0.018\text{ Å}$ ), this suggests that carbon atom C1 should be considered as a carbanion. Ligation of the phosphane arm to the second rhodium atom (Rh2–P1 2.230(1) Å) results in a head-to-tail dimer of overall  $C_2$  symmetry composed of five fused (partly metallacyclic) rings (6–4–6–4–6 in size). Location of the two methine carbons above the P1–P2–Rh1–Rh2 mean plane results in a boat conformation of the central six-membered ring.<sup>[18]</sup> Because of the constrained geometry, the Rh1–N1 bond is significantly shortened relative to **1** (2.096(4) Å in **2** versus 2.171(2) in **1**). The C–O bond is slightly elongated due to the stronger *trans* influence of the hydrocarbonyl ligand relative to the pyridine donor in **1** (Rh1–C33 1.157(7) Å in **2** vs. Rh1–C46 1.143(3) Å in **1**).

The formation of **2** could be envisioned to involve intermediate **I** (Scheme 2), which may be formed by, for example, direct external azide-induced desilylation or inner-sphere azide attack and 1,5-silyl transfer (given the short C–H–Cl distance observed in **1**, this methylene group might be considered a center of reactivity). From **I**, a change in coordination mode of



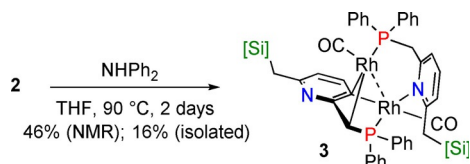
**Scheme 2.** Possible reaction pathway for the formation of dimeric complex **2** involving heterolytic C–Si bond cleavage in the presence of  $\text{NaN}_3$ .

the ligand from  $\kappa^2\text{-P,N}$  to  $\kappa^2\text{-C,N}$  would lead to formation of monomeric four-membered rhodacycle **2M**. This transformation occurs on reaction of group 13 metalloids with external Lewis acids.<sup>[7]</sup> DFT calculations showed that model compound **2M** is only  $15.2\text{ kcal mol}^{-1}$  less stable than **I**, but this difference originates solely from the strain imposed on the bidentate ligand on coordination ( $\Delta\Delta E_{\text{strain}} = 22.3\text{ kcal mol}^{-1}$ , see Supporting Information for details). C,N coordination is in fact favored by  $6.2\text{ kcal mol}^{-1}$  over P,N coordination, which can be rationalized by localization of the negative charge on the carbon atom. This is also reflected in the higher NICS value of  $-8.392$  for **2M** compared to  $-3.900$  in **I**. Eventually, this unsaturated Rh<sup>I</sup> complex dimerizes to generate complex **2** with two square-planar rhodium centers.

Monitoring the conversion of **1** to **2** by  $^{31}\text{P}$  NMR spectroscopy showed an initial stationary period ( $\pm 24\text{ h}$ ) without significant changes preceding sudden formation of a complex mixture, which precluded high-fidelity characterization of relevant intermediates. This mixture ultimately disappeared in favor of selective formation of **2**, which was the only product after 96 h. Attempts to detect a silylazide byproduct were unsuccessful. We reasoned that the same reaction with model compound  $\text{PN}^{\text{Si}}$ , bearing only the silyl group  $[\text{Si}]^{\beta}$  to the phosphane (i.e. 2-[(diphenylphosphanyl)(methyl)diphenylsilyl)methyl]-6-methylpyridine), might provide some mechanistic insight.

Ligand **PN**<sup>Si</sup> was obtained as a colorless oil in modest yield in two steps starting from 2-[(diphenylphosphanyl)methyl]-6-methylpyridine. The corresponding crystalline orange rhodium complex [Rh(CI(CO)(PN<sup>Si</sup>))] (**1**) was also fully characterized, including single-crystal X-ray structure determination (see Supporting Information). The observed Cl1-Rh1-P1 angle of 162.97(4)° and the presence of a C-H-Cl interaction suggest that steric hindrance imposed by the SiMePh<sub>2</sub> fragment is not the main driving force behind this transformation. However, on treatment of **1** with NaN<sub>3</sub> under the same conditions as for **1**, no evidence for formation of analogue **2**' lacking any silyl group was observed, which would be the expected product on direct external attack of azide on the flanking [Si] unit. Hence, this result strongly suggests that the formation of **2** requires the presence of both [Si]<sup>1</sup> and [Si]<sup>2</sup>. This could indicate that the C-H-Cl interaction might be a mechanistically relevant factor for site-specific desilylation. Furthermore, DFT calculations indicate the existence of  $\pi$ -arene coordination of one of the [Si]<sup>2</sup> phenyl groups to the metal center after NaCl elimination in **1**, estimated to be about 7 kcal mol<sup>-1</sup>, which may account for the different reactivity with respect to **1**'. However, a full computational mechanistic study is outside the scope of this report.

Monomeric intermediate **2**<sup>M</sup> (Scheme 2) is a tautomeric form of the previously postulated reactive form of dearomatized PN(P) complexes. We thus wondered whether metal-ligand bifunctional bond activation of, for example, amines to afford formal reprotonation of the methine carbon and coordination of an NR<sub>2</sub> fragment to a mononuclear Rh<sup>I</sup> center would be accessible with **2**.<sup>[19]</sup> Heating an equimolar solution of **2** and diphenylamine in THF at 90 °C in a pressure tube for 2 d led to a color change from yellow to dark red (Scheme 3). Monitoring



Scheme 3. Isomerization of **2** to **3** assisted by diphenylamine.

this reaction by <sup>31</sup>P NMR spectroscopy showed gradual disappearance of complex **2**, concomitant with the formation of two new doublets of doublets of doublets ( $\delta = 17.9, 34.3$  ppm; <sup>1</sup>J<sub>Rh1P1</sub> = 124.1, <sup>1</sup>J<sub>Rh2P2</sub> = 164.6, <sup>2</sup>J<sub>Rh1P2</sub> = 4.5, <sup>2</sup>J<sub>Rh2P1</sub> = 4.5, J<sub>PP</sub> = 17.2 Hz), which suggest retention of a dimeric geometry featuring two inequivalent phosphorus and rhodium nuclei. Although the reaction proceeded cleanly with 46% conversion after 2 d based on the <sup>1</sup>H NMR spectroscopic data, red complex **3** could only be isolated in 16% yield due to its high solubility in a wide range of solvents. Use of triethylamine gave 66% yield (NMR) of **3** in the same timeframe.

The <sup>1</sup>H NMR spectrum of **3** indicated reprotonation of one methine fragment, and the two hydrogen atoms of this CH<sub>2</sub>P methylene unit resonate at  $\delta = 4.22$  and 5.13 ppm. The remaining methine fragment in dimer **3** is strongly deshielded com-

pared with **2** ( $\delta = 4.75$  ppm in **3**;  $\delta = 2.33$  ppm in **2**) and the hydrogen atom couples to both <sup>31</sup>P nuclei and one <sup>103</sup>Rh nucleus; this suggests that some binding interaction between Rh and C persists after reaction with an amine. The use of an additional equivalent of amine per dimer did not change the outcome of this reaction. No nitrogen-based fragment was incorporated in **3** according to CSI-HRMS ([M+H]<sup>+</sup>: m/z 1235.1696) and <sup>13</sup>C NMR spectroscopy. This suggests that complex **3** is merely a constitutional isomer of **2** and that the amine acts as proton shuttle to facilitate the isomerization process. This is in agreement with the higher yield (NMR) on changing NHPH<sub>2</sub> to the more basic NEt<sub>3</sub>. Single crystals suitable for X-ray diffraction analysis (including one equivalent of NHPH<sub>2</sub>) were obtained from slow evaporation of a solution in Et<sub>2</sub>O at room temperature (Figure 4).

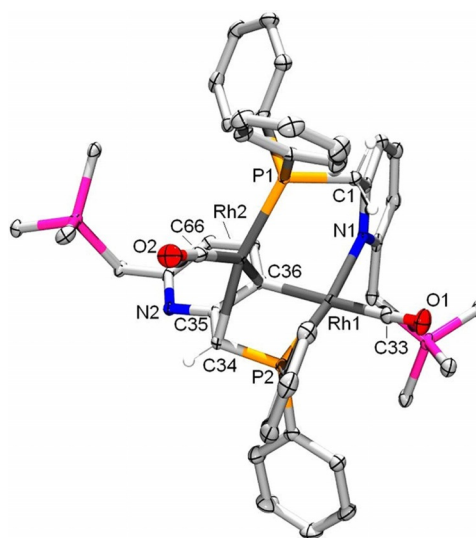
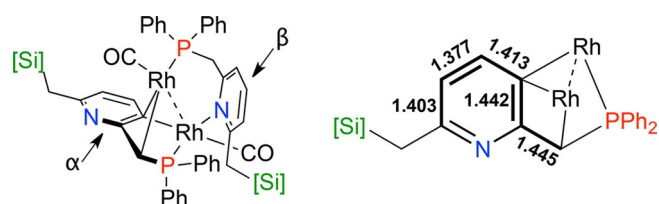


Figure 4. Displacement ellipsoid plots (50% probability) of **3** at 150 K. Hydrogen atoms, apart from those on C1 and C34, and NHPH<sub>2</sub> molecule omitted for clarity. Selected bond lengths [Å] and angles [°]: Rh1–C36 2.166(2); Rh1–N1 2.131(2); Rh1–P2 2.138(6); Rh2–P1 2.2735(6); Rh2–C34 2.168(2); Rh2–C35 2.310(2); Rh2–C36 2.258(2); C34–C35 1.445(2); C35–C36 1.442(3); C34–P2 1.781(2); Rh1–C36–Rh2 79.33(6); C66–Rh2–C34 95.43(8); C66–Rh2–C36 156.48(8); C34–Rh2–C36 66.24(7); P2–Rh1–C36 82.54(5); P2–Rh1–C33 92.51(6); C33–Rh1–C36 170.33(8).

Rather than binding to an anionic methine donor, as found in **2**, rhodium center Rh1 in **3** binds to the C–H-activated, anionic *meta*-carbon atom C36 of the second pyridine fragment (Rh1–C36 2.116(2) Å). Rhodium atom Rh2 binds to carbanion C34 (Rh2–C34 2.168(2) Å) in a  $\sigma$  fashion and to carbon atom C36 in a  $\pi$  interaction (Rh2–C36 2.258(2) Å). Electronic structure analysis showed no bond critical point between Rh2 and C35 (see Supporting Information). The coordination sphere of Rh2 is completed by phosphane P atom P1 of the regenerated –C(1)H<sub>2</sub>PR<sub>2</sub> arm and a CO ligand *trans* to C36, and nitrogen donor N2 is no longer bound to Rh2. The Rh1–Rh2 distance of 2.7942(7) Å is shorter than that in a structurally slightly related dinuclear complex in which one Rh atom is bound in a  $\pi$  fashion to an iminopyridine-derived scaffold (Rh1–Rh2 2.9157(1) Å), likely due to the P,N chelate present in

**3.**<sup>[20]</sup> The coordination mode adopted by the C–H-activated pyridine ring is somewhat similar to the ligation of a bridging hydrocarbyl fragment in an Ni dimer (Ni–Ni 2.710(2) Å).<sup>[21]</sup>

In accordance with the spectroscopic and HRMS data, the highly unusual structure of **3** results from a prototropic isomerization of **2**. This isomerization involves formal deprotonation of the *meta* position of one pyridine ring (heterocycle  $\alpha$ ) by the methine arm of the other pyridine (heterocycle  $\beta$ ), mediated by a proton-shuttling amine. The two heterocycles differ significantly in their electronic structures (Figure 5). Pyridine ring  $\beta$  is aromatic with C–C distances of 1.376–1.392 Å, whereas in ring  $\alpha$  the C–C bond lengths alternate between those of double and single C–C bonds.



**Figure 5.** Left:  $\alpha$  and  $\beta$  heterocycles in **3**. Right: alternating C–C bond lengths in heterocycle  $\alpha$ .

Although a few *meta*-metalated pyridine complexes of Rh<sup>III</sup> have previously been characterized,<sup>[22]</sup> complex **3** is the first such Rh<sup>I</sup> complex that has been structurally characterized in the solid state.<sup>[23]</sup> It is noteworthy that *meta*-pyridine C–H bond metalation is rare, typically involving organolithium reagents<sup>[24]</sup> or harsh conditions.<sup>[25]</sup> In the case of rhodium, a highly reactive 14-electron complex has been reported to undergo C–H oxidative addition of bipyridine-type substrates,<sup>[26]</sup> and [Rh<sup>III</sup>(Cp\*)(C<sub>5</sub>H<sub>5</sub>)(H)(PMe<sub>3</sub>)] reacts with pyridine to afford 15% of the *m*-C–H activation product, together with 57 and 28% of the more reactive *o*-C–H and *p*-C–H activation products, respectively.<sup>[27]</sup> Furthermore, we are not aware of any examples of complexes that feature a  $\sigma,\pi$ -bridging 3-pyridyl ligand.

## Conclusions

We have reported the first examples of *C,N* rather than *P,N* ligation of a reactive *P,N*-type ligand in the coordination sphere of any transition metal (Rh<sup>I</sup>), induced by a site-selective carbon–silicon cleavage strategy with NaN<sub>3</sub>. The carbanionic methine fragment generated in situ displaces phosphorus as donor to Rh<sup>I</sup> to result in a highly strained four-membered Rh–N–C–C metallacycle, stabilized by dimerization involving phosphane coordination to the neighboring rhodium center. Amine-assisted proton shuttling transforms dimer **2** into **3**, which shows an unusual  $\sigma,\pi$ -bridging 3-pyridyl coordination mode. These findings are considered of relevance for the design of new synthetic routes and modes of activity of reactive ligands and the chemistry of cyclometalated rhodium carbanions. We are currently pursuing similar transformations with PN<sup>Si2</sup> and other transition metals and follow-up reactivity therewith.<sup>[28]</sup>

## Experimental Section

### General comments

All reactions and manipulations were carried out under an atmosphere of dry dinitrogen by using standard Schlenk techniques or in a glovebox. All solvents were purged with dinitrogen and dried with an MBraun Solvent Purification System (SPS); <sup>1</sup>H, <sup>13</sup>C, <sup>31</sup>P, <sup>29</sup>Si NMR spectra were recorded with a Bruker AV 300, Bruker DRX 300, Bruker AV 400, or Varian Mercury 300 spectrometer at room temperature unless noted otherwise. Chemical shifts were expressed relative to residual <sup>1</sup>H, <sup>13</sup>C solvent signals, 85% H<sub>3</sub>PO<sub>4</sub>, and external tetramethylsilane, respectively. Mass spectra were recorded with an AccuTOF LC, JMS-T100LP, AccuTOF GC v 4g, or JMS-T100GCV mass spectrometer. IR spectra were recorded with a Bruker Vertex 70v spectrometer. Elemental analyses were carried out by Kolbe Mikroanalytisches Labor, Oberhausen (Germany). (Diphenylphosphanyl)methyl-6-methyl-pyridine was prepared according to a literature procedure.<sup>[29]</sup>

### 2,6-Bis[(diphenylmethylsilyl)methyl]pyridine (A)

Compound **A** was prepared by a slightly modified procedure.<sup>[14a]</sup> A solution of *n*-butyllithium in hexanes (51.6 mL, 2.5 M, 2.07 equiv) was added dropwise to a solution of 1,6-dimethylpyridine (7.22 mL, 62.2 mmol) and tetramethylethylenediamine (19.6 mL, 130.6 mmol, 2.1 equiv) in diethyl ether (200 mL) at 0 °C leading to an intense red solution. The reaction mixture was allowed to warm to room temperature and was further stirred for 5 h. During this time, the color of the solution turned from red to brownish. The solution thus obtained was added dropwise over 45 min to a –90 °C solution of diphenylmethylsilyl chloride (27.2 mL, 128.8 mmol, 2.07 equiv) in diethyl ether (200 mL). The reaction mixture was then allowed to slowly warm to room temperature and stirred for an additional 48 h to give a clear yellow solution and a white precipitate. After removal of the volatile substances under reduced pressure, the solid residue was extracted with diethyl ether and filtered through a plug of activated neutral alumina. The solvent was then removed under reduced pressure to give a yellow oil. After column chromatography on silica gel (eluent Et<sub>2</sub>O/pentane, 20/80; R<sub>f</sub> = 0.46), the compound was obtained as a white solid, which was crystallized at –20 °C from a saturated Et<sub>2</sub>O/pentane solution as white crystals in a yield of 35%. HRMS (ESI, –30 °C): exact mass (monoisotopic) calcd for [C<sub>33</sub>H<sub>33</sub>NSi<sub>2</sub>]<sup>+</sup>: *m/z* 499.2152; found: 499.2171; <sup>1</sup>H NMR (300 MHz, C<sub>6</sub>D<sub>6</sub>):  $\delta$  = 0.53 (s, 6H, CH<sub>3</sub>), 2.84 (s, 4H, CH<sub>2</sub>), 6.32 (d, 2H, <sup>3</sup>J<sub>HH</sub> = 7.61 Hz, H<sub>*m*-py</sub>), 6.76 (t, 1H, <sup>3</sup>J<sub>HH</sub> = 7.61 Hz, H<sub>*p*-py</sub>), 7.14–7.22 (m, 12H, H<sub>Ph</sub>), 7.49–7.57 (m, 8H, H<sub>Ph</sub>); <sup>13</sup>C{<sup>1</sup>H} NMR (76 MHz, C<sub>6</sub>D<sub>6</sub>):  $\delta$  = –3.75 (s, 2C, CH<sub>3</sub>), 27.9 (s, 2C, CH<sub>2</sub>), 118.9 (s, 2C, CH<sub>*m*-py</sub>), 128.1 (s, 8C, CH<sub>Ph</sub>), 129.5 (s, 4C, CH<sub>*p*-Ph</sub>), 135.2 (s, 8C, CH<sub>Ph</sub>), 135.6 (s, 1C, CH<sub>*p*-py</sub>), 137.2 (s, 4C, CH<sub>*o*-Ph</sub>), 159.6 (s, 2C, C<sub>*o*-py</sub>).

### Ligand PN<sup>Si2</sup>

A solution of *n*-butyllithium in hexanes (2.0 mL, 2.5 M, 1.0 equiv) was added dropwise to a suspension of **A** (2.5 g, 5.0 mmol) in diethyl ether (25 mL) at –78 °C. The resulting mixture was then allowed to warm to room temperature and was stirred for 15 min at room temperature to give an orange solution. This solution was then cooled to –78 °C, and chlorodiphenylphosphane (0.92 mL, 5.0 mmol, 1 equiv) was added dropwise at this temperature. The reaction mixture was then allowed to warm to room temperature to give a clear yellow solution and a white precipitate. After filtration through a plug of Celite, the volatile substances were re-

moved under vacuum and the residue was extracted with hexane (2×20 mL) and filtered through a cannula. After removal of the volatile substances under reduced pressure, **2** was obtained as a colorless oil in a yield of 94%. HRMS (FD, −30 °C): exact mass (monoisotopic) calcd for  $[C_{45}H_{42}N_1P_1Si_2]^+$ :  $m/z$  683.25934; found: 683.26875; elemental analysis (%) calcd for  $C_{45}H_{42}NPSi_2$ : C 79.02, H 6.19, N 2.05; found: C 79.23, H 6.36, N 2.11;  $^1H$  NMR (300 MHz,  $CD_2Cl_2$ ):  $\delta$  = 0.44 (s, 3H,  $CH_3$ ), 0.50 (s, 3H,  $CH_3$ ), 2.74 (AB spin system, 2H,  $^2J_{HH}$  = 13.4 Hz,  $CH_2$ ), 4.05 (d, 1H,  $^2J_{HP}$  = 3.4 Hz, HC-P), 6.32 (d, 1H,  $^3J_{HH}$  = 7.6 Hz,  $H_{m-py}$ ), 6.69 (d, 1H,  $^3J_{HH}$  = 7.7 Hz,  $H_{m-py}$ ), 6.96 (pseudo-t, 1H,  $^3J_{HH}$  = 7.7 Hz,  $H_{p-py}$ ), 7.02–7.63 (m, 30H,  $H_{ph}$ );  $^{13}C\{^1H\}$  NMR (76 MHz,  $CD_2Cl_2$ ):  $\delta$  = −4.0 (s, 1C,  $CH_3$ ), −3.5 (d, 1C,  $^3J_{CP}$  = 4.9 Hz,  $CH_3$ ), 27.5 (s, 1C,  $CH_2$ ), 37.4 (d, 1C,  $^1J_{CP}$  = 33.0 Hz, HC-P), 119.2 (d, 1C,  $J_{CP}$  = 1.8 Hz,  $CH_{m-py}$ ), 120.3 (d, 1C,  $J_{CP}$  = 8.5 Hz,  $CH_{m-py}$ ), 127.6 (s, 2C,  $CH_{ph-s}$ ), 127.7 (s, 2C,  $CH_{ph-s}$ ), 128.1 (s, 2C,  $CH_{ph-s}$ ), 128.2 (s, 2C,  $CH_{ph-s}$ ), 128.2 (d, 2C,  $J_{CP}$  = 7.2 Hz,  $CH_{ph-p}$ ), 128.3 (d, 2C,  $J_{CP}$  = 8.0 Hz,  $CH_{ph-p}$ ), 128.4 (s, 1C,  $CH_{ph}$ ), 129.2 (s, 1C,  $CH_{ph-s}$ ), 129.3 (s, 1C,  $CH_{ph-s}$ ), 129.4 (s, 1C,  $CH_{ph-s}$ ), 129.5 (s, 1C,  $CH_{ph-s}$ ), 129.6 (s, 1C,  $CH_{ph-s}$ ), 133.5 (d, 2C,  $^2J_{CP}$  = 20.5 Hz,  $CH_{ph-p}$ ), 134.8 (d, 2C,  $^2J_{CP}$  = 22.5 Hz,  $CH_{ph-p}$ ), 135.1 (s, 2C,  $CH_{ph}$ ), 135.1 (s, 2C,  $CH_{ph}$ ), 135.4 (d, 2C,  $J_{CP}$  = 1.4 Hz,  $CH_{ph}$ ), 135.7 (m, 3C, 2 $CH_{ph}$  and  $CH_{p-py}$ ), 136.2 (d, 1C,  $J_{CP}$  = 2.9 Hz, Si-C<sub>quat</sub>), 136.4 (d, 1C,  $J_{CP}$  = 1.4 Hz, Si-C<sub>quat</sub>), 137.2 (s, 1C, Si-C<sub>quat</sub>), 137.4 (s, 1C, Si-C<sub>quat</sub>), 138.2 (d, 1C,  $J_{CP}$  = 15.3 Hz, P-C<sub>quat</sub>), 139.3 (d, 1C,  $J_{CP}$  = 21.6 Hz, P-C<sub>quat</sub>), 159.6 (s, 1C, C<sub>o-py</sub>), 160.2 (d, 1C,  $J_{CP}$  = 4.4 Hz, C<sub>o-py</sub>);  $^{31}P\{^1H\}$  NMR (121 MHz,  $CD_2Cl_2$ ):  $\delta$  = −9.7 (s);  $^{29}Si\{^1H\}$  NMR (60 MHz,  $CD_2Cl_2$ ):  $\delta$  = −8.2 (d,  $^2J_{SiP}$  = 18.5 Hz, Si<sup>1</sup>), −7.8 (s, Si<sup>2</sup>).

### Ligand PN<sup>Si2</sup>

A solution of *n*-butyllithium in diethyl ether (1.92 mmol, 0.77 mL, 2.5 M, 1 equiv) was added dropwise to a solution of 2-(diphenylphosphanyl)methyl-6-methylpyridine (560 mg, 1.92 mmol) in diethyl ether (20 mL) at −78 °C. Then, the resulting yellow solution was allowed to warm to room temperature and was stirred for an additional 30 min at this temperature to an give orange solution. After cooling this solution to −78 °C, chloromethyldiphenylsilane (404  $\mu$ L, 1.92 mmol, 1 equiv) was added dropwise and the reaction mixture was allowed to warm to room temperature and was stirred for a further 1 h at this temperature. After removal of the volatile substances under reduced pressure, the orange residue was extracted with pentane (2×10 mL), and the extracts were combined and filtered through a plug of neutral alumina, which was then washed with pentane (5 mL) to afford a clear and colorless solution. This solution was concentrated until saturation and stored at −20 °C overnight to precipitate the expected compound as a colorless oil in a yield of 23%. HRMS (FD): exact mass (monoisotopic) calcd for  $[C_{32}H_{30}N_1P_1Si_1]^+$ :  $m/z$  487.18851; found: 487.18183;  $^1H$  NMR (300 MHz,  $CD_2Cl_2$ ):  $\delta$  = 0.45 (s, 3H,  $CH_3$ -Si), 2.32 (s, 3H,  $CH_3$ ), 4.03 (d, 1H,  $^2J_{HP}$  = 3.4 Hz, HC-P), 6.64 (d, 1H,  $^3J_{HH}$  = 7.6 Hz,  $CH_{m-py}$ ), 6.77 (d, 1H,  $^3J_{HH}$  = 7.8 Hz,  $CH_{m-py}$ ), 7.03–7.50 (m, 21H,  $H_{ph}$ );  $^{13}C\{^1H\}$  NMR (76 MHz,  $CD_2Cl_2$ ):  $\delta$  = −3.6 (d, 1C,  $^3J_{CP}$  = 4.8 Hz,  $CH_3$ -Si), 24.3 (s, 1C,  $CH_3$ ), 37.5 (d, 1C,  $^1J_{CP}$  = 33.3 Hz, P-C(H)-Si), 119.1 (d, 1C,  $J_{CP}$  = 2.0 Hz,  $CH_{m-py}$ ), 121.2 (d, 1C,  $J_{CP}$  = 7.8 Hz,  $CH_{m-py}$ ), 127.6 (s, 2C,  $CH_{ph-s}$ ), 127.7 (s, 2C,  $CH_{ph-s}$ ), 128.1 (d, 2C,  $J_{CP}$  = 7.0 Hz,  $CH_{ph-p}$ ), 128.4 (d, 2C,  $J_{CP}$  = 7.8 Hz,  $CH_{ph-p}$ ), 128.5 (s, 1C,  $CH_{ph}$ ), 129.2 (s, 1C,  $CH_{ph}$ ), 129.3 (s, 1C,  $CH_{ph}$ ), 129.3 (brs, 1C,  $CH_{ph}$ ), 133.6 (d, 2C,  $J_{CP}$  = 20.5 Hz,  $CH_{ph-p}$ ), 134.7 (d, 2C,  $J_{CP}$  = 22.4 Hz,  $CH_{ph-p}$ ), 135.3 (d, 2C,  $J_{CP}$  = 1.2 Hz,  $CH_{ph-s}$ ), 135.7 (d, 2C,  $J_{CP}$  = 1.5 Hz,  $CH_{ph-s}$ ), 136.1 (s, 1C,  $CH_{p-py}$ ), 136.3 (d, 1C,  $J_{CP}$  = 2.1 Hz, Si-C<sub>quat</sub>), 138.0 (d, 1C,  $J_{CP}$  = 14.8 Hz, P-C<sub>quat</sub>), 138.9 (d, 1C,  $J_{CP}$  = 20.9 Hz, P-C<sub>quat</sub>), 157.9 (s, 1C, C<sub>o-py</sub>), 160.2 (d, 1C,  $J_{CP}$  = 4.1 Hz, C<sub>o-py</sub>), the signal for one quaternary C atom connected to silicon was not observed;  $^{31}P\{^1H\}$  NMR (121 MHz,  $CD_2Cl_2$ ):  $\delta$  = 8.5;  $^{29}Si\{^1H\}$  NMR (60 MHz,  $CD_2Cl_2$ ):  $\delta$  = −8.3 (d,  $^2J_{SiP}$  = 18.4 Hz).

### [RhCl(CO)( $\kappa^2$ -P,N-PN<sup>Si2</sup>)] (1)

Dichloromethane (10 mL) was added to a mixture of PN<sup>Si2</sup> (536 mg, 0.78 mmol) and  $[[Rh(CO)_2Cl_2]$  (145 mg, 0.37 mmol, 0.475 equiv) at −78 °C and the resulting mixture was allowed to warm to room temperature with stirring to give an orange solution. The complex was then precipitated as a yellow powder by addition of pentane (50 mL), and the mother liquor was removed by filtration. The powder was then dissolved in dichloromethane, and the solution filtered through Celite and layered with pentane to afford the expected complex as yellow crystals in a yield of 47% (with respect to the rhodium complex). Crystals suitable for XRD analysis were obtained by slow diffusion of pentane into a saturated dichloromethane solution of the complex at room temperature. HRMS (FD): exact mass (monoisotopic) calcd for  $[C_{46}H_{42}Cl_1O_1N_1P_1Si_2Rh_1]^+$ :  $m/z$  849.12861; found: 849.12866; elemental analysis (%) calcd for  $C_{46}H_{42}ClINOPRhSi_2$ : C 64.97, H 4.98, N 1.65; found: C 64.97, H 5.02, N 1.64;  $^1H$  NMR (300 MHz,  $CD_2Cl_2$ ):  $\delta$  = 0.05 (s, 3H,  $CH_3$ -Si), 1.21 (s, 3H,  $CH_3$ -Si), 2.97 (d, 1H,  $^2J_{HH}$  = 13.6 Hz,  $CH_2$ ), 4.42 (d, 1H,  $^2J_{HP}$  = 15.6 Hz, HC-P), 5.30 (d, 1H,  $^2J_{HH}$  = 13.6 Hz,  $CH_2$ ), 6.30 (d, 2H,  $^3J_{HH}$  = 7.8 Hz,  $H_{m-py}$ ), 6.82 (t, 1H,  $^3J_{HH}$  = 7.8 Hz,  $H_{p-py}$ ), 6.94–7.04 (m, 2H,  $H_{arom}$ ), 7.08–7.18 (m, 2H,  $H_{arom}$ ), 7.19–7.44 (m, 24H,  $H_{arom}$ ), 7.53–7.63 (m, 2H,  $H_{arom}$ );  $^{13}C\{^1H\}$  NMR (76 MHz,  $CD_2Cl_2$ ):  $\delta$  = −4.1 (s, 1C,  $CH_3$ -Si), −2.9 (s, 1C,  $CH_3$ -Si), 29.5 (s, 1C,  $CH_2$ ), 43.0 (d, 1C,  $^1J_{CP}$  = 15.5 Hz, P-C(H)-Si), 120.1 (d, 1C,  $J_{CP}$  = 9.4 Hz,  $CH_{m-py}$ ), 123.0 (s, 1C,  $CH_{m-py}$ ), 128.0 (s, 2C,  $CH_{ph-s}$ ), 128.1–128.3 (m, 6C,  $CH_{ph-s}$ ), 128.6 (d, 2C,  $J_{CP}$  = 11.2 Hz,  $CH_{ph-p}$ ), 129.1 (d,  $J_{CP}$  = 10.3 Hz,  $CH_{ph-p}$ ), 129.6 (dd, 1C,  $J_{CP}$  = 56.6 Hz,  $J_{CRh}$  = 4.5 Hz, P-C<sub>quat</sub>), 129.6 (s, 1C,  $CH_{ph-s}$ ), 129.7 (s, 1C,  $CH_{ph-s}$ ), 129.8 (s, 1C,  $CH_{ph-s}$ ), 130.0 (s, 1C,  $CH_{ph-s}$ ), 130.4 (d, 1C,  $J_{CP}$  = 2.3 Hz,  $CH_{ph-p}$ ), 131.8 (d, 2C,  $J_{CP}$  = 11.5 Hz,  $CH_{ph-p}$ ), 131.8 (d, 1C,  $J_{CP}$  = 2.7 Hz,  $CH_{ph-p}$ ), 133.5 (s, 1C, Si-C<sub>quat</sub>), 134.1 (d, 1C,  $J_{CP}$  = 40.4 Hz, P-C<sub>quat</sub>), 134.1 (dd, 2C,  $J_{CP}$  = 12.6 Hz,  $J_{CRh}$  = 1.7 Hz,  $CH_{ph-p}$ ), 134.9 (s, 2C,  $CH_{ph-s}$ ), 135.0 (d, 1C,  $J_{CP}$  = 4.9 Hz, Si-C<sub>quat</sub>), 135.1 (s, 2C,  $CH_{ph-s}$ ), 135.3 (s, 2C,  $CH_{ph-s}$ ), 135.4 (s, 2C,  $CH_{ph-s}$ ), 136.1 (s, 1C,  $CH_{p-py}$ ), 162.1 (d, 1C,  $J_{CP}$  = 3.2 Hz, C<sub>o-py</sub>), 165.8 (s, 1C, C<sub>o-py</sub>), 190.4 (dd, 1C,  $J_{CRh}$  = 74.4 Hz,  $J_{CP}$  = 13.8 Hz, CO);  $^{31}P\{^1H\}$  NMR (121 MHz,  $CD_2Cl_2$ ):  $\delta$  = 67.6 (d,  $^1J_{PRh}$  = 167.6 Hz);  $^{29}Si\{^1H\}$  NMR (79 MHz,  $CD_2Cl_2$ ):  $\delta$  = −7.0 (s), −6.7 (brs). IR (ATR mode,  $cm^{-1}$ ):  $\nu$  1987 (s; CO).

### [RhCl(CO)( $\kappa^2$ -P,N-PN<sup>Si</sup>)] (1')

Dichloromethane (5 mL) was added to a mixture of PN<sup>Si</sup> (218 mg, 0.45 mmol) and  $[[Rh(CO)_2Cl_2]$  (86.9 mg, 0.22 mmol, 0.5 equiv) at −78 °C with stirring and the resulting mixture was allowed to warm to room temperature to give an orange solution. The complex was then precipitated as a yellow powder by addition of pentane (20 mL) and the mother liquor was removed by filtration. The powder was then dissolved in dichloromethane (6 mL), and the solution filtered through a cannula and layered with pentane (16 mL) to afford the expected complex as dichloromethane solvate (orange crystals, 63% yield). Crystals suitable for XRD analysis were obtained by slow diffusion of pentane into a saturated dichloromethane solution of the complex at room temperature. HRMS (FD): exact mass (monoisotopic) calcd for  $[C_{33}H_{30}NPRhSi-CO]^+$ :  $m/z$  625.06287; found: 625.09933; elemental analysis (%) calcd for  $C_{33}H_{30}ClINOPRhSi+CH_2Cl_2$ : C 55.26, H 4.36, N 1.90; found: C 55.48, H 4.30, N 1.98;  $^1H$  NMR (300 MHz,  $CD_2Cl_2$ ):  $\delta$  = 0.18 (s, 3H,  $CH_3$ -Si), 3.04 (s, 3H,  $CH_3$ -py), 4.42 (brd, 1H,  $^2J_{HP}$  = 15.0 Hz, CH-P), 6.40 (d, 1H,  $^3J_{HH}$  = 9.0 Hz,  $H_{m-py}$ ), 6.84 (d, 1H,  $^3J_{HH}$  = 9.0 Hz,  $H_{m-py}$ ), 6.97–7.08 (m, 2H,  $H_{arom}$ ), 7.09–7.48 (m, 17H,  $H_{arom}$ ), 7.50–7.61 (m, 2H,  $H_{arom}$ );  $^{13}C\{^1H\}$  NMR (75 MHz,  $CD_2Cl_2$ ):  $\delta$  = −2.7 (s, 1C,  $CH_3$ -Si), 27.9 (s, 1C,  $CH_3$ -py), 43.9 (d, 1C,  $^1J_{CP}$  = 15.8 Hz, P-C(H)-Si), 121.4 (d, 1C,  $J_{CP}$  = 9.0 Hz,  $CH_{m-py}$ ), 123.0 (s, 1C,  $CH_{m-py}$ ), 128.2 (s, 2C,  $CH_{ph-s}$ ), 128.3 (s, 2C,  $CH_{ph-s}$ ), 128.7 (d, 2C,  $J_{CP}$  = 11.3 Hz,  $CH_{ph-p}$ ), 128.9 (d, 2C,  $J_{CP}$  =

10.5 Hz, CH<sub>Ph-P</sub>), 129.5 (dd, 1C, J<sub>CP</sub> = 56.5, J<sub>CRh</sub> = 4.5 Hz, P-C<sub>quat</sub>), 129.9 (s, 1C, CH<sub>Ph-Si</sub>), 130.1 (s, 1C, CH<sub>Ph-Si</sub>), 130.7 (d, 1C, J<sub>CP</sub> = 2.3 Hz, CH<sub>Ph-P</sub>), 131.7 (d, 1C, J<sub>CP</sub> = 3.0 Hz, CH<sub>Ph-P</sub>), 132.6 (brd, 2C, J<sub>CP</sub> = 12.0 Hz, CH<sub>Ph-P</sub>), 133.5 (dd, 2C, J<sub>CP</sub> = 15.0 Hz, J<sub>CRh</sub> = 1.5 Hz, CH<sub>Ph-P</sub>), 133.7 (s, 1C, Si-C<sub>quat</sub>), 134.2 (d, 1C, J<sub>CP</sub> = 39.8 Hz, P-C<sub>quat</sub>), 134.9 (d, 1C, <sup>3</sup>J<sub>CP</sub> = 5.3 Hz, Si-C<sub>quat</sub>), 135.2 (s, 2C, CH<sub>Ph-Si</sub>), 135.4 (s, 2C, CH<sub>Ph-Si</sub>), 138.0 (s, 1C, CH<sub>p-py</sub>), 162.6 (dd, 1C, J<sub>CP</sub> = 3.8 Hz, J<sub>CRh</sub> = 0.8 Hz, C<sub>o-py</sub>), 163.4 (s, 1C, C<sub>o-py</sub>), 190.5 (dd, 1C, J<sub>CRh</sub> = 74.3 Hz, J<sub>CP</sub> = 13.5 Hz, CO). <sup>31</sup>P{<sup>1</sup>H} NMR (121 MHz, CD<sub>2</sub>Cl<sub>2</sub>): δ = 70.1 (d, <sup>1</sup>J<sub>PRh</sub> = 164.6 Hz); <sup>29</sup>Si{<sup>1</sup>H} NMR (60 MHz, CD<sub>2</sub>Cl<sub>2</sub>): δ = -7.3 (d, <sup>2</sup>J<sub>SiP</sub> = 3.0 Hz).

### [Rh<sup>I</sup>(CO)(κ<sup>2</sup>-N,C;κ<sup>1</sup>-P-μ-PN<sup>5</sup>)]<sub>2</sub> (2)

THF (13 mL) was added to a mixture of **1** (186.5 mg, 0.22 mmol) and sodium azide (90.0 mg, 1.38 mmol, 6.3 equiv) in a Schlenk vessel kept away from light and the resulting suspension was stirred at room temperature for 4 d to give a brown reaction mixture. The <sup>31</sup>P{<sup>1</sup>H} NMR analysis of the crude mixture showed the disappearance of the starting material and the quantitative formation of a new species resonating at δ = 47.2 ppm in THF. The crude mixture was filtered through Celite and slightly concentrated (to 10 mL), and pentane (20 mL) was added to precipitate a yellow powder. After elimination of the mother liquor by filtration, the powder was dissolved in THF (5 mL) and the solution was filtered to give a very limpid solution. This solution was layered with pentane (13 mL) to afford **2** as yellow crystals (containing two molecules of THF per complex) in 37% yield; elemental analysis (%) calcd for [C<sub>66</sub>H<sub>58</sub>N<sub>2</sub>O<sub>2</sub>P<sub>2</sub>O<sub>2</sub>Rh<sub>2</sub>Si<sub>2</sub>+2THF]: C 64.44, H 5.41, N 2.03; found: C 64.62, H 5.58, N 2.07; <sup>1</sup>H NMR (300 MHz, [D<sub>8</sub>]THF): δ = 0.30 (s, 6H, CH<sub>3</sub>-Si), 2.33 (br, 2H, HC-P), 2.65 (AB spin system, 4H, <sup>2</sup>J<sub>HH</sub> = 15.0 Hz, CH<sub>2</sub>), 6.36 (d, 2H, J<sub>HH</sub> = 6.0 Hz, CH<sub>py</sub>), 6.41 (d, 2H, J<sub>HH</sub> = 9.0 Hz, CH<sub>py</sub>), 7.08–7.38 (m, 24H, H<sub>arom.</sub>), 7.39–7.48 (m, 4H, H<sub>arom.</sub>), 7.50–7.61 (m, 2H, H<sub>arom.</sub>), 7.73–7.84 (m, 2H, H<sub>arom.</sub>); <sup>13</sup>C{<sup>1</sup>H} NMR: due to the very low resolution of the spectrum, assignment was not possible; <sup>31</sup>P{<sup>1</sup>H} NMR (121 MHz, [D<sub>8</sub>]THF): δ = 45.7; <sup>29</sup>Si{<sup>1</sup>H} NMR (79 MHz, [D<sub>8</sub>]THF): δ = -9.3(s); IR (ATR, cm<sup>-1</sup>): ν̄ = 1947 (s, CO).

### Isomerization of **2** to form complex **3**

**Method 1:** THF (5.0 mL) was added to a mixture of **2** (360 mg, 0.290 mmol) and diphenylamine (46.9 mg, 0.277 mmol, 0.95 equiv) in a vessel with J. Young valve suitable for reactions under pressure. The resulting suspension was heated to 90 °C for 48 h to give a dark red solution (NMR yield 46%, internal standard dichloroethane). After removal of the volatile substances under reduced pressure, the residue was extracted with diethyl ether (5 mL), and the solution filtered and concentrated until saturation. Storing this solution at -20 °C afforded a dark red mixture of **3** and HNPh<sub>2</sub> (1/0.69) in 16% yield. Crystals suitable for XRD were obtained by slow evaporation of a saturated diethyl ether solution at room temperature; the crystal lattice contains one molecule of diphenylamine

**Method 2:** An NMR tube containing a solution of **2** (20 mg, 14.5 μmol) and trimethylamine (2.0 μL, 14.5 μmol, 1 equiv) in [D<sub>8</sub>]THF was heated at 90 °C. Monitoring of the reaction by <sup>1</sup>H NMR spectroscopy showed complete conversion after 25 h with a yield of 66%, determined by integration of the signal of one SiMe group relative to the Me group of toluene as internal standard (V<sub>tol</sub> = 2 μL, D1 relaxation time = 10 s).

**Data for **2**:** HRMS (ESI, -43 °C): m/z: exact mass (monoisotopic) calcd for [C<sub>66</sub>H<sub>58</sub>N<sub>2</sub>O<sub>2</sub>P<sub>2</sub>Si<sub>2</sub>Rh<sub>2</sub>+H]<sup>+</sup>: 1235.1700; found: 1235.1696; <sup>1</sup>H NMR (300 MHz, CD<sub>2</sub>Cl<sub>2</sub>): δ = 0.5 (s, 3H, CH<sub>3</sub>-Siβ), 0.58 (s, 3H, CH<sub>3</sub>-Siα), 2.70 [AB system ΔV<sub>AB</sub> = 13.4 Hz]: 2.68 (1H, <sup>2</sup>J<sub>HH</sub> = 12.9 Hz, Si-CH<sub>2</sub>α), 2.72 (1H, <sup>2</sup>J<sub>HH</sub> = 12.9 Hz, Si-CH<sub>2</sub>α), 2.81 (d, 1H, <sup>2</sup>J<sub>HH</sub> = 13.9 Hz, CH<sub>2</sub>-Siβ), 4.02 (d, 1H, <sup>2</sup>J<sub>HH</sub> = 13.9 Hz, CH<sub>2</sub>-Siβ), 4.22 (dd, 1H, <sup>2</sup>J<sub>HH</sub> =

12.0, <sup>2</sup>J<sub>HP</sub> = 12.0 Hz, CH<sub>2</sub>-Pβ), 4.75 (pseudo-dt, 1H, <sup>1</sup>J<sub>PH</sub> = 4.3, <sup>2</sup>J<sub>HP</sub> = 4.3, <sup>1</sup>J<sub>RhH</sub> = 2.7 Hz, HC-Rh), 5.13 (dd, 1H, <sup>2</sup>J<sub>HH</sub> = 12.0, <sup>2</sup>J<sub>PH</sub> = 6.3 Hz, CH<sub>2</sub>-Pβ), 5.65 (d, 1H, <sup>3</sup>J<sub>HH</sub> = 7.9 Hz, CH<sub>py</sub>α), 5.98 (d, 1H, <sup>3</sup>J<sub>HH</sub> = 7.9 Hz, CH<sub>py</sub>α), 6.58 (d, 1H, <sup>3</sup>J<sub>HH</sub> = 7.9 Hz, CH<sub>m-py</sub>β), 6.64 (d, 1H, <sup>3</sup>J<sub>HH</sub> = 7.8 Hz, CH<sub>m-py</sub>β), 7.03–7.61 (m, 37H, H<sub>arom.</sub>), 7.78 (m, 2H, H<sub>arom.</sub>), 8.04 (m, 2H, H<sub>arom.</sub>); <sup>13</sup>C{<sup>1</sup>H} NMR (76 MHz, CD<sub>2</sub>Cl<sub>2</sub>): δ = -4.1 (s, 1C, CH<sub>3</sub>-Si), -3.5 (s, 1C, CH<sub>3</sub>-Si), 28.7 (s, 1C, CH<sub>2</sub>-Siα), 32.8 (s, 1C, CH<sub>2</sub>-Siβ), 41.1 (br, 1C, HC-Rh), 45.5 (brd, 1C, <sup>1</sup>J<sub>PC</sub> = 21.0 Hz, CH<sub>2</sub>-Pβ), 117.2 (brs, 1C, CH<sub>py</sub>α), 122.8 (brs, 1C, CH<sub>m-py</sub>β), 123.9 (brs, 1C, CH<sub>m-py</sub>β), 127.8 (d, 2C, J<sub>PC</sub> = 11.4 Hz, CH<sub>Ph-P</sub>), 127.9 (s, 2C, CH<sub>Ph-Si</sub>), 128.0 (brd, 2C, J<sub>PC</sub> = 10.6 Hz, CH<sub>Ph-P</sub>), 128.1 (s, 2C, CH<sub>Ph-Si</sub>), 128.4 (s, 2C, CH<sub>Ph-Si</sub>), 128.5 (s, 2C, CH<sub>Ph-Si</sub>), 128.6 (d, 2C, J<sub>PC</sub> = 8.8 Hz, CH<sub>Ph-P</sub>), 128.7 (d, 2C, J<sub>PC</sub> = 9.5 Hz, CH<sub>Ph-P</sub>), 129.1 (brs, 1C, CH<sub>Ph</sub>), 129.3 (s, 1C, CH<sub>Ph</sub>), 129.4 (d, 1C, J<sub>PC</sub> = 2.5 Hz, CH<sub>p-Ph-P</sub>), 129.5 (s, 1C, CH<sub>Ph</sub>), 129.8 (s, 1C, CH<sub>Ph</sub>), 130.1 (s, 1C, CH<sub>Ph</sub>), 130.2 (brs, 1C, CH<sub>Ph</sub>), 130.3 (d, 2C, J<sub>PC</sub> = 10.2 Hz, CH<sub>Ph-P</sub>), 130.9 (d, 1C, J<sub>PC</sub> = 2.0 Hz, CH<sub>p-Ph-P</sub>), 132.9 (d, 2C, J<sub>PC</sub> = 10.9 Hz, CH<sub>Ph-P</sub>), 134.5 (dd, 2C, J<sub>PC</sub> = 10.2 Hz, J<sub>RhC</sub> = 1.5 Hz, CH<sub>Ph-P</sub>), 134.7 (s, 2C, CH<sub>Ph-Si</sub>), 135.1 (s, 2C, CH<sub>Ph-Si</sub>), 135.1 (s, 2C, CH<sub>Ph-Si</sub>), 135.3 (s, 2C, CH<sub>Ph-Si</sub>), 135.4 (s, C<sub>quat</sub>), 136.3 (brd, 2C, J<sub>PC</sub> = 15.1 Hz, CH<sub>Ph-P</sub>), 136.3 (s, 1C, C<sub>quat</sub>), 136.4 (brd, <sup>1</sup>J<sub>PC</sub> = 64.6 Hz, C<sub>Ph-P</sub>), 137.0 (s, 1C, C<sub>quat</sub>), 137.2 (s, 1C, C<sub>quat</sub>), 137.4 (d, 1C, J<sub>PC</sub> = 1.5 Hz, CH<sub>p-py</sub>β), 143.1 (dd, J<sub>PC</sub> = 41.0 Hz, J<sub>RhC</sub> = 1.4 Hz, C<sub>Ph-P</sub>), 151.9 (br, 1C, C<sub>quat</sub>), 153.7 (s, 1C, CH<sub>py</sub>α), 157.5 (d, 1C, J<sub>PC</sub> = 4.1 Hz, C<sub>quat</sub>), 163.0 (d, 1C, J<sub>PC</sub> = 2.0 Hz, C<sub>quat</sub>), 163.8 (s, 1C, C<sub>quat</sub>), 191.4–193.1 (br, 2C, CO); the signal of the C atom connected to rhodium in the *meta* position of the N heterocycle was not observed; <sup>31</sup>P{<sup>1</sup>H} NMR (121 MHz, CD<sub>2</sub>Cl<sub>2</sub>): δ = 17.9 (ddd, <sup>1</sup>J<sub>RhP</sub> = 124.1 Hz, J = 17.2 Hz, J = 4.5 Hz), 34.3 (ddd, <sup>1</sup>J<sub>RhP</sub> = 164.6 Hz, J = 17.2 Hz, J = 4.5 Hz); <sup>29</sup>Si{<sup>1</sup>H} NMR (79 MHz, CD<sub>2</sub>Cl<sub>2</sub>): δ = -8.2 (br, Siα and Siβ), detected by means of a 2D HSQC [<sup>1</sup>H, <sup>29</sup>Si] experiment.

### X-ray crystallography

**Complexes **1** and **2**:** All reflection intensities were measured with a Bruker D8 Quest Eco diffractometer equipped with a Triumph monochromator (λ = 0.71073 Å) and a CMOS Photon 50 detector at 150(2) K. Intensity data were integrated with the Bruker APEX2 software.<sup>[30]</sup> Absorption correction and scaling were performed with SADABS.<sup>[31]</sup> The structures were solved by intrinsic phasing with the program SHELXT.<sup>[30]</sup> Least-squares refinement was performed with SHELXL-2013<sup>[32]</sup> against F<sup>2</sup> of all reflections. Non-hydrogen atoms were refined with anisotropic displacement parameters. The H atoms were placed at calculated positions by using the instruction AFIX 13, AFIX 43, or AFIX 137 with isotropic displacement parameters having 1.2 or 1.5 U<sub>eq</sub> of the attached C atoms. For complex **2**, the contribution of disordered THF lattice solvent was removed from the final refinement by using the SQUEEZE procedure.<sup>[33]</sup>

**Complex **3**:** All reflection intensities were measured at 110(2) K with a SuperNova diffractometer equipped with an Atlas detector and Mo<sub>Kα</sub> radiation (λ = 0.71073 Å) by using the program CrysAlis-Pro (Version 1.171.36.32, Agilent Technologies, 2013 or Version 1.171.38.41, Rigaku OD, 2015). The same program was used to refine the cell dimensions and for data reduction. The structure was solved with the program SHELXS-2014/7 and was refined on F<sup>2</sup> with SHELXL-2014/7.<sup>[34]</sup> Numerical absorption correction based on Gaussian integration or analytical numeric absorption correction over a multifaceted crystal model was applied by using CrysAlisPro. The temperature of the data collection was controlled with a Cryojet system (Oxford Instruments). The H atoms were placed at calculated positions (unless otherwise specified) by using the instructions AFIX 43, AFIX 123, AFIX 137, or AFIX 147 with isotropic displacement parameters having 1.2 or 1.5 U<sub>eq</sub> of the attached C or O atoms.



CCDC 1590066, 1590067 and 1589141 contain the supplementary crystallographic data for this paper. These data are provided free of charge by The Cambridge Crystallographic Data Centre.

### DFT calculations

Density functional calculations were performed at the  $\omega$ B97X-D<sup>[35]</sup> level of theory by using Gaussian 09, revision D.01.<sup>[36]</sup> Geometry optimizations were performed with the DEF2TZVP basis set<sup>[37]</sup> and frequency calculations were performed to ensure minima on the potential-energy surface. NICS values<sup>[38]</sup> were calculated by the GIAO method<sup>[39]</sup> at the B3LYP/6-31G(d,p) level of theory.<sup>[40,41]</sup> The interaction energy of the Rh(CO)Cl fragment in the different coordination modes of **1** and **2M** was determined with respect to the ligand in the geometry of the complexes. The Topological Analysis of the Electron Density<sup>[42]</sup> was performed by using ADF<sup>[43]</sup> at the  $\omega$ B97X-D/TZ2P level of theory including relativistic effects with the Zeroth Order Regular Approximation (ZORA).<sup>[44]</sup> Phenyl groups were replaced by methyl groups to limit the computation time.

### Acknowledgements

This research has been funded through ERC Starting Grant 27097 (EuReCat). We thank Prof. Bas de Bruin for fruitful discussions and Ed Zuidinga and Jan-Meine Ernsting for assistance with MS and NMR analysis, respectively.

### Conflict of interest

The authors declare no conflict of interest.

**Keywords:** C–H activation • coordination modes • metallacycles • N,P ligands • rhodium

- [1] a) C. Gunanathan, D. Milstein, *Acc. Chem. Res.* **2011**, *44*, 588–602; b) J. I. van der Vlugt, *Eur. J. Inorg. Chem.* **2012**, 363–375; c) B. Zhao, Z. Han, K. Ding, *Angew. Chem. Int. Ed.* **2013**, *52*, 4744–4788; *Angew. Chem.* **2013**, *125*, 4844–4889; d) J. R. Khushnutdinova, D. Milstein, *Angew. Chem. Int. Ed.* **2015**, *54*, 12236–12273; e) R. H. Morris, *Acc. Chem. Res.* **2015**, *48*, 1494–1502; f) J. I. van der Vlugt, *Chem. Eur. J.* **2019**, DOI: <https://doi.org/10.1002/chem.201802606>.
- [2] a) J. I. van der Vlugt, J. N. H. Reek, *Angew. Chem. Int. Ed.* **2009**, *48*, 8832–8846; *Angew. Chem.* **2009**, *121*, 8990–9004; b) C. Gunanathan, D. Milstein, *Chem. Rev.* **2014**, *114*, 12024–12087; c) H. Li, B. Zheng, K.-W. Huang, *Coord. Chem. Rev.* **2015**, *293*–294, 116–138.
- [3] Recent contributions: a) E. Fogler, J. A. Garg, P. Hu, G. Leitus, L. J. W. Shimon, D. Milstein, *Chem. Eur. J.* **2014**, *20*, 15727–15731; b) Y. Gloaguen, C. Rebreyend, M. Lutz, P. Kumar, M. Huber, J. I. van der Vlugt, S. Schneider, B. de Bruin, *Angew. Chem. Int. Ed.* **2014**, *53*, 6814–6818; *Angew. Chem.* **2014**, *126*, 6932–6936; c) M. Glatz, B. Bichler, M. Mastalir, B. Stöger, M. Weil, K. Mereiter, E. Pittenauer, G. Allmaier, L. F. Veiros, K. Kirchner, *Dalton Trans.* **2015**, *44*, 281–294; d) S. Perdriau, D. S. Zijlstra, H. J. Heeres, J. G. De Vries, E. Otten, *Angew. Chem. Int. Ed.* **2015**, *54*, 4236–4240; *Angew. Chem.* **2015**, *127*, 4310–4314; e) H. Taguchi, D. Sasaki, K. Takeuchi, S. Tsujimoto, T. Matsuo, H. Tanaka, K. Yoshizawa, F. Ozawa, *Organometallics* **2016**, *35*, 1526–1533; f) T. Simler, P. Braunstein, A. A. Danopoulos, *Organometallics* **2016**, *35*, 4044–4049; g) C. Hou, J. Jiang, Y. Li, C. Zhao, Z. Ke, *ACS Catal.* **2017**, *7*, 786–795; h) A. V. Polezhaev, C.-H. Chen, Y. Losovyj, K. G. Caulton, *Chem. Eur. J.* **2017**, *23*, 8039–8050; i) G. R. Morello, K. H. Hopmann, *ACS Catal.* **2017**, *7*, 5847–5855; j) P. Daw, Y. Ben-David, D. Milstein, *ACS Catal.* **2017**, *7*, 7456–7460; k) J. J. Gair, Y. Qiu, N. H. Chan, A. S. Filatov, J. C. Lewis, *Organometallics* **2017**, *36*, 4699–4706; l) A. Bruneau-Voisine, D. Wang, V. Dorcet, T.

- Roisnel, C. Darcel, J.-B. Sortais, *J. Catal.* **2017**, *347*, 57–62; m) C. Rebreyend, Y. Gloaguen, M. Lutz, J. I. van der Vlugt, I. Siewert, S. Schneider, B. de Bruin, *Chem. Eur. J.* **2017**, *23*, 17438–17441; n) R. Zeng, M. Feller, Y. Ben-David, D. Milstein, *J. Am. Chem. Soc.* **2017**, *139*, 5720–5723; o) F. Freitag, T. Irrgang, R. Kempe, *Chem. Eur. J.* **2017**, *23*, 12110–12113; p) J. A. Luque-Urrutia, A. Poater, *Inorg. Chem.* **2017**, *56*, 14383–14387; q) T. P. Gonçalves, K.-W. Huang, *J. Am. Chem. Soc.* **2017**, *139*, 13442–13449; r) A. Brzozowska, L. M. Azofra, V. Zubar, I. Atodiressei, L. Cavallo, M. Rueping, O. El-Sepelgy, *ACS Catal.* **2018**, *8*, 4103–4109; s) M. Glatz, B. Stöger, D. Himmelbauer, L. F. Veiros, K. Kirchner, *ACS Catal.* **2018**, *8*, 4009–4016; t) R. Zeng, M. Feller, Y. Diskin-Posner, L. J. W. Shimon, Y. Ben-David, D. Milstein, *J. Am. Chem. Soc.* **2018**, *140*, 7061–7064; u) C. P. Yap, Y. Y. Chong, T. S. Chwee, W. Y. Fan, *Dalton Trans.* **2018**, *47*, 8483–8488; v) L. Li, M. Lei, L. Liu, Y. Xie, H. F. Schaefer, *Inorg. Chem.* **2018**, *57*, 8778–8787; w) Y.-Q. Zou, S. Chakraborty, A. Nerush, D. Oren, Y. Diskin-Posner, Y. Ben-David, D. Milstein, *ACS Catal.* **2018**, *8*, 8014–8019; x) T. Cheisson, L. Mazaud, A. Auffrant, *Dalton Trans.* **2018**, *47*, 14521–14530; y) C. Guan, Y. Pan, E. P. L. Ang, J. Hu, C. Yao, M.-H. Huang, H. Li, Z. Lai, K.-W. Huang, *Green Chem.* **2018**, *20*, 4201–4205; z) H. Li, A. Al-Dakhil, D. Lupp, S. Gholap, S. Z. Lai, L.-C. Liang, K.-W. Huang, *Org. Lett.* **2018**, *20*, 6430–6435.
- [4] Work from our group: a) J. I. van der Vlugt, E. A. Pidko, D. Vogt, M. Lutz, A. L. Spek, A. Meetsma, *Inorg. Chem.* **2008**, *47*, 4442–4444; b) J. I. van der Vlugt, E. A. Pidko, D. Vogt, M. Lutz, A. L. Spek, *Inorg. Chem.* **2009**, *48*, 7513–7515; c) J. I. van der Vlugt, M. Lutz, E. A. Pidko, D. Vogt, A. L. Spek, *Dalton Trans.* **2009**, 1016–1023; d) J. I. van der Vlugt, M. A. Siegler, M. Janssen, D. Vogt, A. L. Spek, *Organometallics* **2009**, *28*, 7025–7032; e) L. S. Jongbloed, B. de Bruin, J. N. H. Reek, M. Lutz, J. I. van der Vlugt, *Chem. Eur. J.* **2015**, *21*, 7297–7305; f) Z. Tang, E. Otten, J. N. H. Reek, J. I. van der Vlugt, B. de Bruin, *Chem. Eur. J.* **2015**, *21*, 12683–12693; g) S. Y. de Boer, T. J. Korstanje, S. R. La Rooij, R. Kox, J. N. H. Reek, J. I. van der Vlugt, *Organometallics* **2017**, *36*, 1541–1549.
- [5] a) J. I. van der Vlugt, E. A. Pidko, R. C. Bauer, Y. Gloaguen, M. K. Rong, M. Lutz, *Chem. Eur. J.* **2011**, *17*, 3850–3854; b) S. Y. de Boer, Y. Gloaguen, M. Lutz, J. I. van der Vlugt, *Inorg. Chim. Acta* **2012**, *380*, 336–342; c) R. C. Handford, B. O. Patrick, P. Legzdins, *Inorg. Chem.* **2017**, *56*, 12641–12651; d) V. Cherepakhin, T. J. Williams, *ACS Catal.* **2018**, *8*, 3754–3763; e) D. Wei, A. Bruneau-Voisine, T. Chauvin, V. Dorcet, T. Roisnel, D. A. Valyaev, N. Lukan, J.-B. Sortais, *Adv. Synth. Catal.* **2018**, *360*, 676–681; f) Y. Hameed, B. Gabidullin, D. Richeson, *Inorg. Chem.* **2018**, *57*, 13092–13096.
- [6] Original observation: a) A. Sacco, G. Vasapollo, C. F. Nobile, A. Piergiovanni, M. A. Pellinghelli, M. Lanfranchi, *J. Organomet. Chem.* **1988**, *356*, 397–409. b) First applications for substrate bond activation and catalysis: J. Zhang, G. Leitus, Y. Ben-David, D. Milstein, *J. Am. Chem. Soc.* **2005**, *127*, 10840–10841; c) J. Zhang, G. Leitus, Y. Ben-David, D. Milstein, *Angew. Chem. Int. Ed.* **2006**, *45*, 1113–1115; *Angew. Chem.* **2006**, *118*, 1131–1133.
- [7] Isolated case for Zr<sup>IV</sup>, with [P,C,N]<sup>2-</sup> coordination: T. Simler, G. Frison, P. Braunstein, A. A. Danopoulos, *Dalton Trans.* **2016**, *45*, 2800–2804.
- [8] M. Devillard, C. Alvarez Lamsfus, V. Vreeken, L. Maron, J. I. van der Vlugt, *Dalton Trans.* **2016**, *45*, 10989–10998.
- [9] R. Kempe, *Eur. J. Inorg. Chem.* **2003**, 791–803.
- [10] a) K. Higashimura, Y. Nakamura, *J. Chem. Soc. Dalton Trans.* **1993**, 3075–3080; b) N. Shinkawa, A. Sato, J. Shinya, Y. Nakamura, S. Okeya, *Bull. Chem. Soc. Jpn.* **1995**, *68*, 183–190; c) K. Yamasaki, H. Saito, M. Tado-koro, K. Matsumoto, S. Miyajima, Y. Nakamura, *Bull. Chem. Soc. Jpn.* **1997**, *70*, 2155–2166.
- [11] Recent examples: a) D. Getty, K. I. Goldberg, *Organometallics* **2001**, *20*, 2545–2551; b) J. R. Krumper, M. Gerisch, A. Magistrato, U. Rothlisberger, R. G. Bergman, T. D. Tilley, *J. Am. Chem. Soc.* **2004**, *126*, 12492–12502; c) A. A. Koridze, A. V. Polezhaev, S. V. Safronov, A. M. Sheloumov, F. M. Dolgushin, M. G. Ezermitskaya, B. V. Lokshin, P. V. Petrovskii, A. S. Peregu-dov, *Organometallics* **2010**, *29*, 4360–4368; d) S. Musa, R. Romm, C. Azerraf, S. Kozuch, D. Gelman, *Dalton Trans.* **2011**, *40*, 8760–8763; e) Y. Gloaguen, L. M. Jongens, J. N. H. Reek, M. Lutz, B. de Bruin, J. I. van der Vlugt, *Organometallics* **2013**, *32*, 4284–4291; f) Y. Gloaguen, W. Jacobs, B. de Bruin, M. Lutz, J. I. van der Vlugt, *Inorg. Chem.* **2013**, *52*, 1682–1684; g) K. J. Jonasson, A. V. Polukeev, R. Marcos, M. S. G. Ahlquist, O. F. Wendt, *Angew. Chem. Int. Ed.* **2015**, *54*, 9372–9375; *Angew. Chem.* **2015**, *127*, 9504–9507; h) L. E. Doyle, W. E. Piers, J. Borau-Garcia, *J. Am.*

- Chem. Soc.* **2015**, *137*, 2187–2190; i) P. Cui, M. R. Hoffbauer, M. Vyushkova, V. Iluc, *Chem. Sci.* **2016**, *7*, 4444–4579; j) K.-S. Feichtner, V. H. Gessner, *Chem. Commun.* **2018**, *54*, 6540–6553.
- [12] a) L. S. Jongbloed, D. García-López, R. van Heck, M. A. Siegler, J. J. Carbó, J. I. van der Vlugt, *Inorg. Chem.* **2016**, *55*, 8041–8047; b) L. S. Jongbloed, B. de Bruin, J. N. H. Reek, M. Lutz, J. I. van der Vlugt, *Catal. Sci. Technol.* **2016**, *6*, 1320–1327; c) L. S. Jongbloed, A. Vogt, N. Sandleben, B. de Bruin, A. Klein, J. I. van der Vlugt, *Eur. J. Inorg. Chem.* **2018**, 2408–2418.
- [13] a) P. Steenwinkel, S. L. James, D. M. Grove, H. Kooijman, A. L. Spek, G. van Koten, *Organometallics* **1997**, *16*, 513–515; b) B. G. Fullmer, H. Fan, M. Pink, J. C. Huffman, N. P. Tsvetkov, K. G. Caulton, *J. Am. Chem. Soc.* **2011**, *133*, 2571–2582; c) G. K. Min, D. Hernández, T. Skrydstrup, *Acc. Chem. Res.* **2013**, *46*, 457–470.
- [14] a) T. Komuro, H. Tobita, *Chem. Commun.* **2010**, *46*, 1136–1137. b) For related mono-hydrosilane substituted pyridines and their reactivity in metal-free CO cleavage, see: M. Devillard, B. de Bruin, M. A. Siegler, J. I. van der Vlugt, *Chem. Eur. J.* **2017**, *23*, 13628–13632.
- [15] Topological analysis of the electron density proved the existence of a bond path and bond critical point between the hydrogen and chlorine atoms, accompanied by a ring critical point for model compound 1-Me (see Supporting Information for details).
- [16] One possible structure of the resulting cationic species could feature  $\pi$ -arene coordination of one Ph group of the SiMePh<sub>2</sub> fragment to the unsaturated Rh<sup>I</sup> center: V. F. Kuznetsov, G. A. Facey, G. P. A. Yap, H. Alper, *Organometallics* **1999**, *18*, 4706–4711.
- [17] Related pyridino-carbyl  $\kappa^2$ -N,C coordination to Cd, Zn, and Hg: a) T. R. van den Ancker, L. M. Engelhardt, M. J. Anderson, G. E. Jacobsen, C. L. Raston, B. W. Skelton, A. H. White, *J. Organomet. Chem.* **2004**, *689*, 1991–1999. Coordination to P, As and Sb: b) T. R. van den Ancker, P. C. Andrews, S. J. King, J. E. McGrady, C. L. Raston, B. A. Roberts, B. W. Skelton, A. H. White, *J. Organomet. Chem.* **2000**, *607*, 213–221.
- [18] Related phosphinamido and sulfonamidophosphanyl structures: a) F. W. Patureau, S. de Boer, M. Kuil, J. Meeuwissen, P.-A. R. Breuil, M. A. Siegler, A. L. Spek, A. J. Sandee, B. de Bruin, J. N. H. Reek, *J. Am. Chem. Soc.* **2009**, *131*, 6683–6685; b) R. Mathialagan, S. Kuppuswamy, A. T. De Denko, M. W. Bezpalko, B. M. Foxman, C. M. Thomas, *Inorg. Chem.* **2013**, *52*, 701–706; c) S. Oldenhof, M. Lutz, B. de Bruin, J. I. van der Vlugt, J. N. H. Reek, *Organometallics* **2014**, *33*, 7293–7298.
- [19] For recent work on metal–ligand cooperative activation of N–H bonds, see: a) E. Khaskin, M. A. Iron, L. J. W. Shimon, J. Zhang, D. Milstein, *J. Am. Chem. Soc.* **2010**, *132*, 8542–8543; b) M. Feller, Y. Diskin-Posner, L. J. W. Shimon, E. Ben-Ari, D. Milstein, *Organometallics* **2012**, *31*, 4083–4101; c) S. Y. de Boer, Y. Gloaguen, J. N. H. Reek, M. Lutz, J. I. van der Vlugt, *Dalton Trans.* **2012**, *41*, 11276–11283; d) T. W. Myers, L. A. Berben, *J. Am. Chem. Soc.* **2013**, *135*, 9988–9990; e) D. V. Gutsulyak, W. E. Piers, J. Borau-García, M. Parvez, *J. Am. Chem. Soc.* **2013**, *135*, 11776–11779; f) Y.-H. Chang, Y. Nakajima, H. Tanaka, K. Yoshizawa, F. Ozawa, *J. Am. Chem. Soc.* **2013**, *135*, 11791–11794. See also: g) R. M. Brown, J. Borau-García, J. Valjus, C. J. Roberts, H. M. Tuononen, M. Parvez, R. Roesler, *Angew. Chem. Int. Ed.* **2015**, *54*, 6274–6277; *Angew. Chem.* **2015**, *127*, 6372–6375; h) G. W. Margulieux, M. J. Bezdek, Z. R. Turner, P. J. Chirik, *J. Am. Chem. Soc.* **2017**, *139*, 6110–6113.
- [20] a) Z. Tang, C. Tejel, M. Martínez de Sarasa Buchaca, M. Lutz, J. I. van der Vlugt, B. de Bruin, *Eur. J. Inorg. Chem.* **2016**, 963–974. See also: b) C. Tejel, M. P. del Río, L. Asensio, F. J. van den Bruele, M. A. Ciriano, N. Tsi-chlis i Spithas, D. G. H. Hetterscheid, B. de Bruin, *Inorg. Chem.* **2011**, *50*, 7524–7534; c) C. Tejel, M. A. Ciriano, M. P. del Río, F. J. van den Bruele, D. G. H. Hetterscheid, N. Tsi-chlis i Spithas, B. de Bruin, *J. Am. Chem. Soc.* **2008**, *130*, 5844–5845.
- [21] J. Cámpora, J. A. López, P. Palma, C. Ruiz, E. Carmona, *Organometallics* **1997**, *16*, 2709–2718.
- [22] a) B. Procacci, R. J. Blagg, R. N. Perutz, N. Rendoñ, A. C. Whitwood, *Organometallics* **2014**, *33*, 45–52; b) B. Procacci, Y. Jiao, M. E. Evans, W. D. Jones, R. N. Perutz, A. C. Whitwood, *J. Am. Chem. Soc.* **2015**, *137*, 1258–1272.
- [23] Solution-state characterization: a) B. L. Booth, R. N. Haszeldine, I. Perkins, *J. Chem. Soc. A* **1971**, 927–929; b) A. J. Deeming, I. P. Rothwell, M. B. Hursthouse, K. M. A. Malik, *J. Chem. Soc. Dalton Trans.* **1979**, 1899–1911; c) K. A. Manbeck, W. W. Brennessel, W. D. Jones, *Inorg. Chim. Acta* **2013**, *397*, 140–143.
- [24] G. Queguiner, F. Marsias, V. Snieckus, J. Epsztajn, *Adv. Heterocycl. Chem.* **1991**, *52*, 187–304.
- [25] a) E. C. Constable, *J. Chem. Soc. Dalton Trans.* **1985**, 1719–1721; b) L. Chu, M. Shang, K. Tanaka, Q. Chen, N. Pissarnitski, E. Streckfuss, J.-Q. Yu, *ACS Cent. Sci.* **2015**, *1*, 394–399; c) Y. Kuninobu, H. Ida, M. Nishi, M. Kanai, *Nat. Chem.* **2015**, *7*, 712–717.
- [26] E. C. Keske, B. D. Moore, O. V. Zenkina, R. Wang, G. Schatte, C. M. Cruden, *Chem. Commun.* **2014**, *50*, 9883–9886.
- [27] W. D. Jones, L. Dong, A. W. Myers, *Organometallics* **1995**, *14*, 855–861.
- [28] We have preliminary data showing that similar  $\kappa^2$ -C,N coordination and dimerization chemistry is available for Ni<sup>II</sup>.
- [29] H. Yang, N. Lukan, R. Mathieu, *Organometallics* **1997**, *16*, 2089–2095.
- [30] Bruker, APEX2 software, Madison WI, USA, **2014**.
- [31] G. M. Sheldrick, SADABS, Universität Göttingen, Germany, **2008**.
- [32] G. M. Sheldrick, SHELXL2013, University of Göttingen, Germany, **2013**.
- [33] A. L. Spek, *Acta Crystallogr. Sect. D* **2009**, *65*, 148–155.
- [34] G. M. Sheldrick, *Acta Crystallogr. Sect. C* **2015**, *71*, 3–8.
- [35] J.-D. Chai, M. Head-Gordon, *Phys. Chem. Chem. Phys.* **2008**, *10*, 6615–6620.
- [36] Gaussian 09, Revision D.01: M. J. Frisch, G. W. Trucks, H. B. Schlegel, G. E. Scuseria, M. A. Robb, J. R. Cheeseman, G. Scalmani, V. Barone, B. Men-nucci, G. A. Petersson, H. Nakatsuji, M. Caricato, X. Li, H. P. Hratchian, A. F. Izmaylov, J. Bloino, G. Zheng, J. L. Sonnenberg, M. Hada, M. Ehara, K. Toyota, R. Fukuda, J. Hasegawa, M. Ishida, T. Nakajima, Y. Honda, O. Kitao, H. Nakai, T. Vreven, J. A. Montgomery, Jr., J. E. Peralta, F. Ogliaro, M. Bearpark, J. J. Heyd, E. Brothers, K. N. Kudin, V. N. Staroverov, T. Keith, R. Kobayashi, J. Normand, K. Raghavachari, A. Rendell, J. C. Burant, S. S. Iyengar, J. Tomasi, M. Cossi, N. Rega, J. M. Millam, M. Klene, J. E. Knox, J. B. Cross, V. Bakken, C. Adamo, J. Jaramillo, R. Gomperts, R. E. Strat-mann, O. Yazyev, A. J. Austin, R. Cammi, C. Pomelli, J. W. Ochterski, R. L. Martin, K. Morokuma, V. G. Zakrzewski, G. A. Voth, P. Salvador, J. J. Dan-nenberg, S. Dapprich, A. D. Daniels, O. Farkas, J. B. Foresman, J. V. Ortiz, J. Cioslowski, D. J. Fox, Gaussian, Inc., Wallingford CT, **2013**.
- [37] a) F. Weigend, R. Ahlrichs, *Phys. Chem. Chem. Phys.* **2005**, *7*, 3297–3305; b) F. Weigend, *Phys. Chem. Chem. Phys.* **2006**, *8*, 1057–1065.
- [38] Z. Chen, C. S. Wannere, C. Corminboeuf, R. Puchta, P. von Ragué Schley-er, *Chem. Rev.* **2005**, *105*, 3842–3888.
- [39] K. Wolinski, J. F. Hilton, P. Pulay, *J. Am. Chem. Soc.* **1990**, *112*, 8251–8260.
- [40] a) R. Ditchfield, W. J. Hehre, J. A. Pople, *J. Chem. Phys.* **1971**, *54*, 724–728; b) W. J. Hehre, R. Ditchfield, J. A. Pople, *J. Chem. Phys.* **1972**, *56*, 2257–2261; c) P. C. Hariharan, J. A. Pople, *Theor. Chim. Acta* **1973**, *28*, 213–222; d) P. C. Hariharan, J. A. Pople, *Mol. Phys.* **1974**, *27*, 209–214; e) M. S. Gordon, *Chem. Phys. Lett.* **1980**, *76*, 163–168; f) M. M. Francl, W. J. Pietro, W. J. Hehre, J. S. Binkley, M. S. Gordon, D. J. DeFrees, J. A. Pople, *J. Chem. Phys.* **1982**, *77*, 3654–3665; g) C. Binning, Jr., L. A. Curtiss, *J. Comput. Chem.* **1990**, *11*, 1206–1216; h) J.-P. Blaudeau, M. P. McGrath, L. A. Curtiss, L. Radom, *J. Chem. Phys.* **1997**, *107*, 5016–5021; i) V. A. Rassolov, J. A. Pople, M. A. Ratner, T. L. Windus, *J. Chem. Phys.* **1998**, *109*, 1223–1229; j) V. A. Rassolov, M. A. Ratner, J. A. Pople, P. C. Redfern, L. A. Curtiss, *J. Comput. Chem.* **2001**, *22*, 976–984.
- [41] For the polarization functions, see: M. J. Frisch, J. A. Pople, J. S. Binkley, *J. Chem. Phys.* **1984**, *80*, 3265–3269.
- [42] a) R. F. W. Bader, *Atoms in Molecules: A Quantum Theory*, Oxford University Press, Oxford, **1994**; b) R. F. W. Bader, *Chem. Rev.* **1991**, *91*, 893–928; c) J. I. Rodríguez, *J. Comput. Chem.* **2013**, *34*, 681–686.
- [43] G. te Velde, F. M. Bickelhaupt, E. J. Baerends, C. Fonseca Guerra, S. J. A. van Gisbergen, J. G. Snijders, T. Ziegler, *J. Comput. Chem.* **2001**, *22*, 931–967.
- [44] E. van Lenthe, A. W. Ehlers, E. J. Baerends, *J. Chem. Phys.* **1999**, *110*, 8943–8953.

Manuscript received: November 2, 2018

Revised manuscript received: December 12, 2018

Accepted manuscript online: January 2, 2019

Version of record online: February 12, 2019